CHAPTER: 5

OPTICAL AND ELECTRICAL PROPERTIES OF $InSb_{1-X}Bi_X$ (X= 0.00, 0.03, 0.04, 0.05) CRYSTALS AND THIN FILMS

I. INTRODUCTION

Among optical studies of solid materials, reflection, absorption, transmission and the relevant optical constants constitute the most significant studies, both in theoretical and experimental areas. Very remarkably useful optical characteristics have emerged due to such investigations for development of complex multilayer optical devices as well as simple monolayer ones structured out of thin films of prospective materials that also contribute to furthering of understanding and harvesting material properties in general both in scientific and industrial interests. In addition, such optical studies prove very valuable in analysing the electronic structure of solids.

Electronic energy band structures of semiconducting solids can also be very reliably determined with the use of optical study results. The thin film optical properties differ from those of corresponding bulk solids to large or greater extent. These differences occur mostly due to microstructure of thin films and in special cases due to physical dimensions, as in nano thin films. The absorption study becomes especially useful when the incident radiation is chosen in a selective range of wavelength.

There are various methods established for evaluating optical constants. These are Abbe's method, optical spectroscopy method, critical angle method and polarimetric method being the most important among them [1-4]. However, the spectroscopy method is the most widely employed method. Specifically, for band structure studies, optical absorption spectroscopy is practically an indispensable yet the simplest and the most direct method.

In literature a few reports are to be found on the optical characterization of bulk crystals and thin films of $InSb_{1-x}Bi_x$ [5-7]. Optical absorption study on Bridgman method grown $InSb_{1-x}Bi_x$ crystals has been reported by Mohan et al [6]. Whereas, similar studies have been reported by Oszwaldowski et al [7] but on the thin films of InSb-Bi obtained using the specialized technique of Flash Evaporation

In the field of optoelectronics, the phenomenon of photoconductivity used in a broad spectrum of applications, involves optical absorption, usually of UV, visible or IR radiations and resulting charge carrier excitation from valence band states to higher energy conduction band states wherein they can freely contribute to electrical conduction. The interaction process may complete with return

of charge carriers to their ground states. These processes are fairly sensitive to material structure and hence also depend on the type and concentration of impurity and structural imperfections present in the material. Theoretically all semiconductors and insulators are photoconductors in principle. However, the free charge carrier life time and capture cross sections play typical roles for the photoconductivity to be significant. When the material is exposed to suitable radiations, the conductivity increases but such materials in which the increase in conductivity is fairly high and useful is not large in number. Quite a number of reports are found in literature on transport properties such as thermoelectricity of InSb [8-9]. However scarce or no reports are found on photoconductivity of thin films of InSb:Bi system. The author has carried out photoconductivity measurements on thin films of $InSb_{1-x}Bi_x$ (x= 0.00, 0.03, 0.04, 0.05) prepared in the laboratory. The results obtained are presented below, following a general introduction to the phenomenon.

II. GENERAL DISCUSSION:

When a photon incident on a semiconductor has its energy of the order of the band gap of the semiconductor or higher, it gets absorbed and a valence band electron gets excited into the conduction band. The valence band states are nearly fully occupied and hence it has quite many electrons whereas the opposite is true for the conduction band; that is, most of the band states are unoccupied with only quite a few states at its bottom occupied. The probability of an electron getting excited from its valence band state to conduction band is therefore high since there are ample empty states available in the conduction band which can be occupied by the transiting electron. This causes highly probable absorption of photon with such energy. When an electron is excited to the conduction band by optical absorption, it may gain more energy than conduction band electrons, which almost all occupy states around E_c, the conduction band edge (figure 1). Of course it may not be so if the semiconductor is heavily doped, which is usually not the case. Due to this excessive energy acquired by it, the excited electron most frequently would release the energy through its lattice interaction, namely, electron-phonon scattering, for reaching thermal equilibrium with the rest of the pre-existing conduction band electrons. The empty states (holes) left in the valence band by the migrating electrons and the migrated electrons in the conduction band together form what are known as electron-hole pairs serve as excess charge carriers to participate in conduction. The excess carriers so produced are therefore out of balance with the environment and hence tend to recombine eventually. The excess carriers being in their respective bands – holes in valence band and electrons in conduction band-make themselves freely available for electrical conduction. This obviously increases the conductivity.

If the incident photon energy is less than the band gap, it cannot excite valence band electrons to conduction band. So in absence of impurity levels in the band gap, the excitation becomes more difficult in pure semiconductors resulting into negligible or no absorption of photons. As a result, some materials are transparent in particular incident photon wavelength ranges, allowing us to' see through' them. Examples are certain insulators like rock salt and ionic crystals of the like, wherein the energy band gap is large enough and is unsurmountable by optical photons. When the band gap value lies around 2eV or more, only longer wavelength light in IR and some red tail radiation of the spectrum can pass through and such materials do appear transparent to such radiations. Beyond 2eV and typically 3eV and more photon energy, the visible range also transmits through. Some common semiconductor band gaps corresponding to various spectral ranges are enlisted in the schematic layout given below (figure 2).

When a photon beam of energy more than the band gap is incident on the semiconductor, there will be absorption exhibited by the resulting spectrum. The relative intensity absorbed depends on the sample thickness as well as on the incident photon energy. The fraction of transmitted of incident intensity that is transmitted can be obtained from the relation:

$$I = I_0 \, e^{-\alpha t}$$

α being the absorption coefficient (characteristic of the material), I_0 the incident intensity and I the transmitted intensity. The absorption coefficient α near the absorption edge of the spectrum can be expressed in terms of the band gap energy E_g as [10]:

$$\alpha \sim (h\upsilon - E_g)^{\gamma}$$

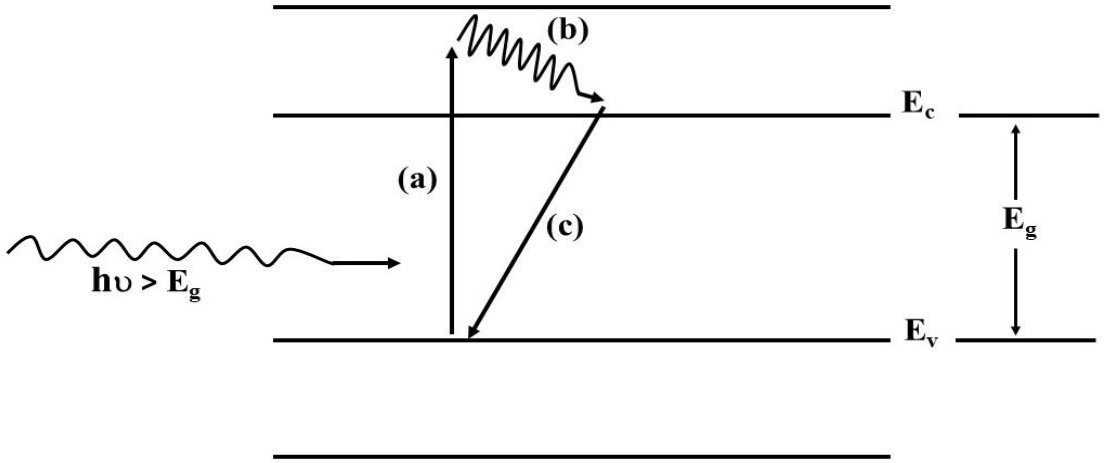

Figure-1 Valence and conduction bands

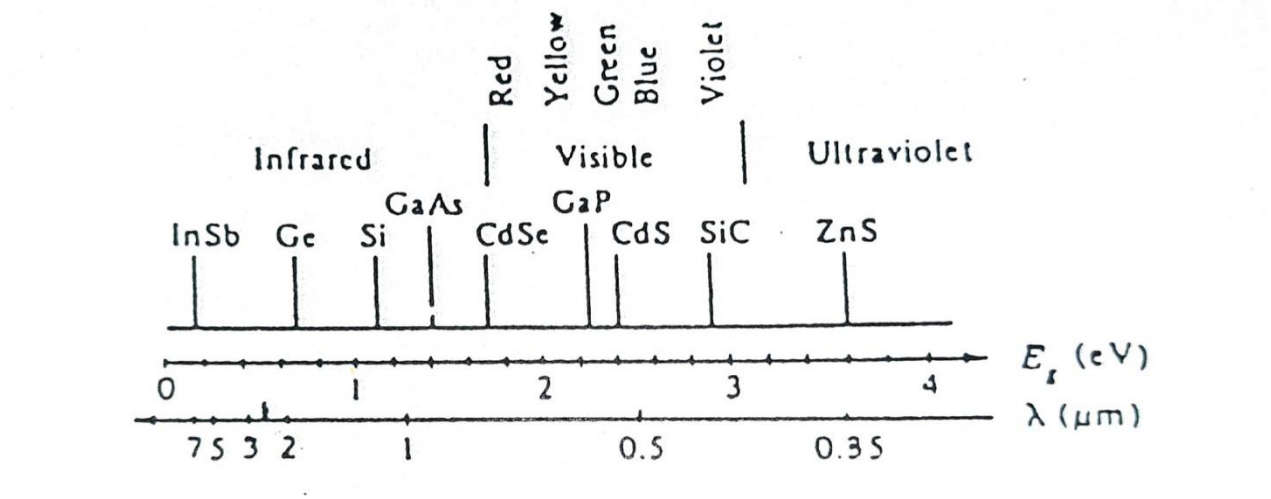

Figure-2 Band gaps of some common semiconductors

where, hυ is the photon energy (familiar expression), γ is a numerical constant which equals $\frac{1}{2}$ and $\frac{3}{2}$ for allowed and forbidden direct transitions, respectively.

The figure 3 illustrates these with K(min) = K(max) at transitions indicated by (a) and (b), respectively. K's here are phonon wave vector magnitudes. It assumes the value 2 in the case of indirect transition, (c), in the figure. In this latter case, lattice interaction with the electron partakes in assisting the transition. For allowed indirect transition, which occurs via exciton states, this constant γ again assumes the value, $\frac{1}{2}$. An exciton is a bound electron–hole pair, which can move through the crystal as a single unit with its ground state energy value lying within the gap region of the band scheme. In all, there can be a number of possible types of transitions that can take place, namely,

interband and intraband. Between impurity states and a band, free carrier transitions within a band and lattice vibration supported transitions involving impurity levels.

The relative rate of decrease in incident intensity with distance across its passage in the sample being examined is defined as the absorption coefficient of a substance. As a result, the coefficient is defined as the relative rate of decrease in light intensity L(hυ) along the propagation path:

$$\alpha\ (h\upsilon) = \frac{1}{L(h\upsilon)} \frac{d(h\upsilon)}{dx}$$

where L(hυ) is incident light intensity of photon energy hν, x the distance traversed by light in the medium. [11].

The electronic transitions in solids were first theorised by Barden et al [12]. The direct transitions are those that occur when an electron transits from the valence to conduction band without change in its crystal momentum signified by its wave vector K. Thus before and after transitions, its wave vector remains the same in such transitions. So direct transitions follow the so called selection rule:

$$K - K' + \frac{2\pi i}{\lambda} = 0$$

where K and K' are respectively the initial and final wave vectors of the electron in the transition process, i stands for the unit vector along its incidence direction and λ is photon wavelength. Since the quantity 2π/ λ is quite small (λ being the light wavelength) compared to magnitudes of the wave vectors, the relation simply becomes (though, strictly an approximation) K' = K. This implies that the only and the most probable transitions allowed will be vertical transitions. Other transitions if at all they occur will have quite small probability of occurrence. The steep linear character of the absorption spectrum near cut off corresponds to highly probable direct allowed transitions. Whereas, the weaker tail in the spectrum corresponds to transitions assisted by phonons, the transitions being hence called indirect transitions due to change in wave vector due to momentum transfer to or from the phonons. In such transitions therefore the initial and final wave vectors do not coincide as a result of this interaction.

The absorption coefficient α as a function of the photon energy and expressed by the equation $\alpha h\upsilon = B\ (h\upsilon - E_g)^x$ applies to direct transitions. Here $x = \frac{1}{2}$ and $x = \frac{3}{2}$ in the cases of allowed and forbidden transitions, respectively, and B is a transition probability dependent parameter.

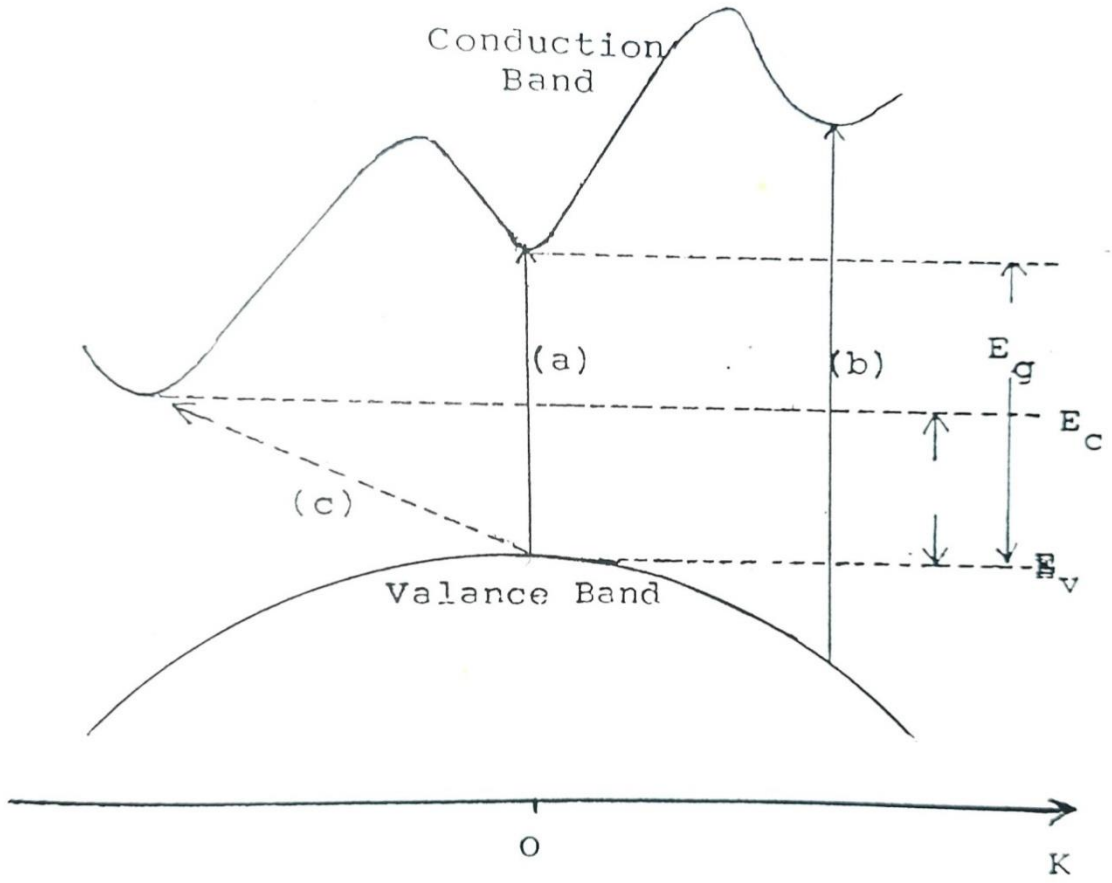

Figure-3 Schematic diagram of energy bands and wave vectors

For indirect transitions, $\alpha h\upsilon = A\,(h\upsilon - E_g \pm E_p)^x$, where x=2 for allowed transitions and x=3 for forbidden transitions and E_p is the absorbed (or emitted) phonon energy [13,14,15]. These transitions, at normal temperatures are accompanied by phonon absorption/emission.

Photoconductivity:

When suitable optical beam of light is made incident on a solid surface, the light may get absorbed to more or less extent and excite electrons in the solid from their stable ground states to higher energy states and several possibilities result. One possibility is that the electrons already in the conduction band, upon excitation by the absorbed light, contribute to increased electrical conductivity. The effect then is termed as photoconductivity. The corresponding photocurrent would obviously depend upon the incident energy and intensity of the illuminating light and to some extent on temperature if it is varied over a range. However, if the excited electrons (e. g., those excited from valence to conduction band), release the acquired excess energy by emission of yet another set of photons and relax to their ground states, such an emission is known as luminescence.

Electronically active solids may be used for storage of energy by employing a basic phenomenon often observed in imperfect crystals and known as trapping of charge carriers. The energy storage is achieved by the spatially so locating a carrier that its free movement through the crystal until external thermal or optical energy is further supplied. When a trapped carrier, an electron or hole, is thus released to move freely, it may again be captured by yet another trap or the so called recombination centre. These agents capable of capturing the carriers and restricting their movement in a confined volume are known in general as traps. Thus there are two classes of capturing centres [16].

1. **Trapping Centre:** If the captured carrier getting re-excited to its free state with thermal energy has a probability greater than that of its recombining with an oppositely charged carrier, the centre is designated as a trapping centre.
2. **Recombination Centre:** On the other hand, we have a 'recombination centre' if the probability of the captured carrier recombining with an oppositely charged carrier (for example, at a site of crystal defect) is greater than the probability of being re-excited to its free state. Although, a centre with its energy level lying near a band edge will most likely behave as a trapping centre than as a recombination centre. The reverse will be true for the centres with their energy levels lying deep in the band gap region. The difference between traps and recombination centres is based on the relative probabilities of the mechanisms of thermal re-excitation and of recombination taking place. Nevertheless, a centre acting as a recombination centra in one condition of incident light intensity and of temperature may behave like a trap in yet other such conditions.

A photoconductor quality is usually determined in terms of photosensitivity defined as change in conductivity per unit excitation intensity.

When light of suitable energy is made incident on a photo conducting material, electron hole pairs generate at equal rates and do also recombine via discrete states like recombination centres which are often impurity states in the material. Such states are almost always above the Fermi level but near the conduction band, so that electrons trapped by them get easily re-excited thermally to the conduction band empty states. Such states that are thermally in equilibrium with electrons in the conduction band come to be known as shallow traps. On the other hand, electrons trapped to deeper lying states in the band gap region cannot easily get thermally excited to an extent that they remain so for quite longer times. In such cases, until sufficient thermal excitation takes place, the trapped electron may capture a free hole and form an exciton. These types of deeper lying states thus act as recombination centres. The prevailing kinetic conditions of the trapping states would determine their occupancy, particularly the condition of their thermal equilibrium or non-equilibrium with the conduction band electrons or with the valence band holes. The demarcation

level that can separate the trapping and the re-combination states has been intricately defined by Bube [17] in terms of distribution of states.

In the case of radiative recombination or capture processes that tend to interrupt or even terminate photosensitivity, luminescence type emission results. Therefore, luminescence measurements can provide valuable information regarding the photosensitivity mechanism.

As per the Scharnhorst model [18] the temperature dependent photosensitivity is governed by the relation $\Delta\sigma(T) \propto \mu_0 n_0(T) = \mu\Delta n$ (where Δn = excess electron concentration, n_0 = the equilibrium electron concentration, μ = the carrier mobility and $\Delta\sigma(T)$ = photosensitivity). A maximum in $\Delta\sigma(T)$ would occur regardless of the given illumination intensity,

The demarcation levels mentioned above was used by Rose [19] for explaining dependence of photosensitivity on temperature and incident illumination intensity. While the discrete states between the two demarcation levels govern the recombination speed, the discrete states beyond the two demarcation levels bear insignificant effect on recombination. The demarcation levels almost always coincide with the Fermi levels or the quasi-Fermi levels, which also determine the electron and hole concentrations in the bands. The charge carrier densities in the band increase with the generation rate of non-equilibrium carriers, eventually causing displacement of the quasi-Fermi levels towards the respective edges of the bands. As a result, the levels acting as traps under weak excitation transform as recombination centres. Conversely, with decreasing generation rate of non-equilibrium carriers, the carrier density decreases causing the quasi-Fermi levels approach one another eventually assuming their equilibrium position, the levels from their status as recombination levels transform into traps under intense excitation.

Under weak excitation, the densities of the free carriers being low compared to their densities in their respective bands, the total bound carrier density effectively remains constant. However, due to intermediate band to band transitions or to these levels, the localized carriers get re-distributed among the recombination and the trap levels.

III. EXPERIMENTAL RESULTS:

The results of optical absorption investigations and band gaps determined are presented in the following sections.

3.1 Band gap of $InSb_{1-x}Bi_x$ (x = 0.00, 0.03, 0.04, 0.05) crystals:

In the wave number range of 500 cm^{-1} to 4000 cm^{-1}, optical absorption was measured and recorded. Using the above-mentioned optical absorption spectra, the absorption coefficient was computed as a function of photon energy. In the palletted samples, the material thickness was assumed to be arbitrary; hence it was not possible to measure the absolute absorption coefficient. However, the relative absorption coefficient was sufficient for the purpose of evaluating band gap. The optical band gaps were evaluated by using the comparison of $(\alpha h\upsilon)^2$ as a function of $h\upsilon$. These band gap plots for $InSb_{1-x}Bi_x$ (x = 0.00, 0.03, 0.04, 0.05) crystals are shown in figures 4, 5, 6 and 7, respectively. In the region of strong fundamental absorption edge, the plots were found to be linear. As a result, the band gap was calculated by projecting (extrapolating) the linear portion to $h\upsilon=0$. The band gap values obtained in this study are listed in table 1.

Table 1: Band gap of $InSb_{1-x}Bi_x$ (x = 0.00, 0.03, 0.04, 0.05) crystals

Crystals	Band gap (eV)
InSb	0.184
$InSb_{0.97}Bi_{0.03}$	0.164
$InSb_{0.96}Bi_{0.04}$	0.171
$InSb_{0.95}Bi_{0.05}$	0.169

3.2 Band gap of $InSb_{1-x}Bi_x$ (x = 0.00, 0.03, 0.04, 0.05) films:

Thin films of $InSb_{1-x}Bi_x$ (x = 0.00, 0.03, 0.04, 0.05) were grown by thermal evaporation technique at room temperature. Films were grown at pressure of 10^{-5} Pa and using quartz crystal monitor film thickness were measured. The comparison of $(\alpha h\upsilon)^2$ as a function of $h\upsilon$ as obtained for $InSb_{1-x}Bi_x$ (x = 0.00, 0.03, 0.04, 0.05) films of thicknesses around 1500 Å are given in figures 8, 9,10 and 11, respectively. The thicknesses of other thin films were plotted in the same way, and the band gaps were calculated. Figures 12, 13, 14, and 15 indicate that the band gap varies as the inverse square of the film thickness, for $InSb_{1-x}Bi_x$ (x = 0.00, 0.03, 0.04, 0.05) respectively. The values of the band

gaps obtained for $InSb_{1-x}Bi_x$ (x = 0.00, 0.03, 0.04, 0.05) thin films are given in tables 2, 3, 4 and 5 respectively.

It is seen that the band gap decreases with increase of thin film thickness. The quantum size effect helps explain the thickness dependency of the band gap. The band gap variation with film thickness follows the relation [20]

$$E_z = \frac{\hbar^2\pi^2}{2m^*}\frac{1}{t^2}$$

The linear variation of E_g vs $1/t^2$ can be explained in terms of quantum size effect. This is commonly characterised as the relationship between a solid's physical qualities and its geometric dimensions. These dimensions are comparable to the charge carriers' de Broglie wavelength. [21, 22]. The transverse component of quasi-momentum is quantized due to the decrease in the band gap. Therefore, in the thin films, the electron-hole states assume quasi-discrete energy values. As a result, the spacing between the valence and conduction bands increases by an amount ΔE, as determined by the aforementioned relationship. The slope of the E_g vs $1/t^2$ plot is used to calculate the effective mass of charge carriers (assuming that electrons are heavy) is found to be 17.488×10^{-4} m_0, 18.402×10^{-4} m_0, 23.29×10^{-4} m_0 and 33.36×10^{-4} m_0 in $InSb_{1-x}Bi_x$ (x = 0.00, 0.03, 0.04, 0.05) respectively, where m_0 is the electron rest mass.

The de Broglie wavelength of holes, calculated using fermi energy assumed to be half of the average bandgap, turns out to be about 102.8nm, 107nm, 93.6nm and 78.23nm in $InSb_{1-x}Bi_x$ (x = 0.00, 0.03, 0.04, 0.05) respectively. This gives rise to quantum size effect in the film with thickness in the range used, viz., 525Å to 1509Å, 500Å to 1503Å, 505Å to 1503Å and 512Å 1512Å respectively. Therefore, the thin films clearly exhibit the quantum size effect.

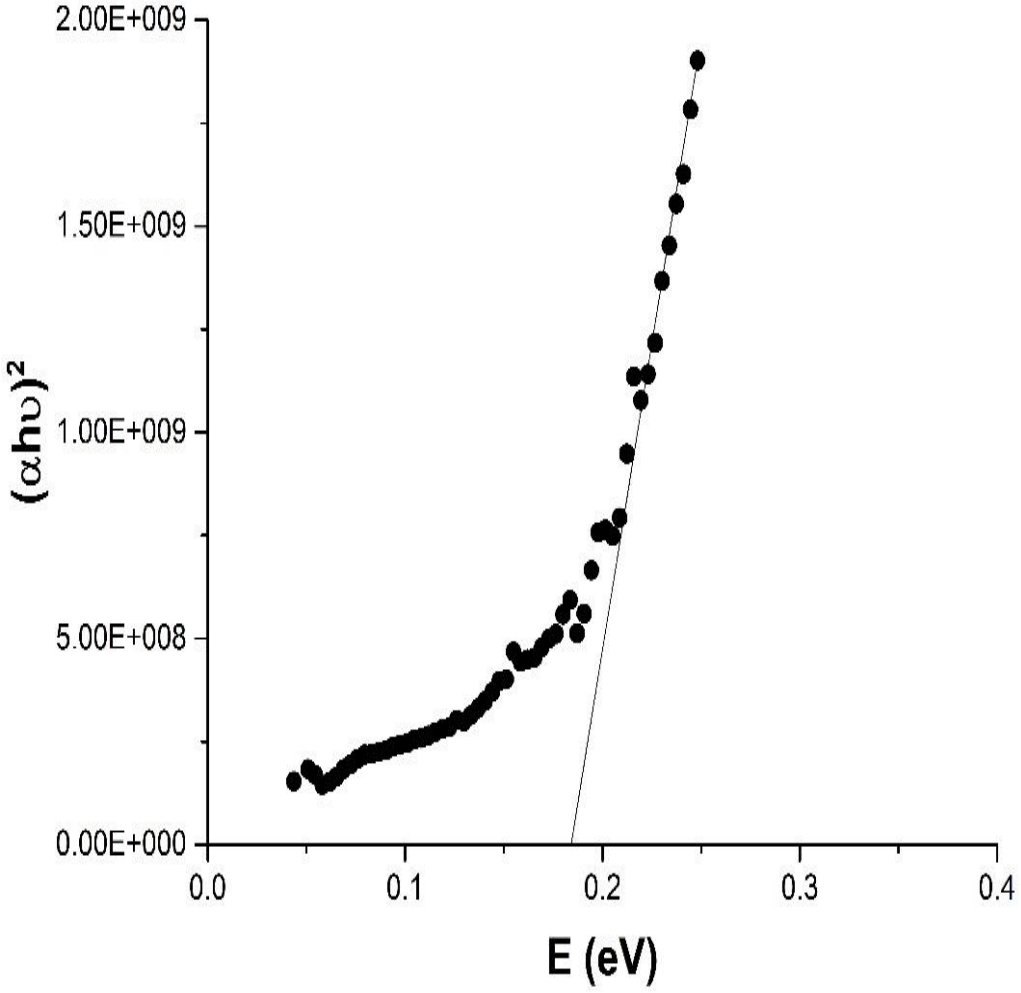

Figure- 4 Plot of $(\alpha h\upsilon)^2$ versus $h\upsilon$ of InSb crystal

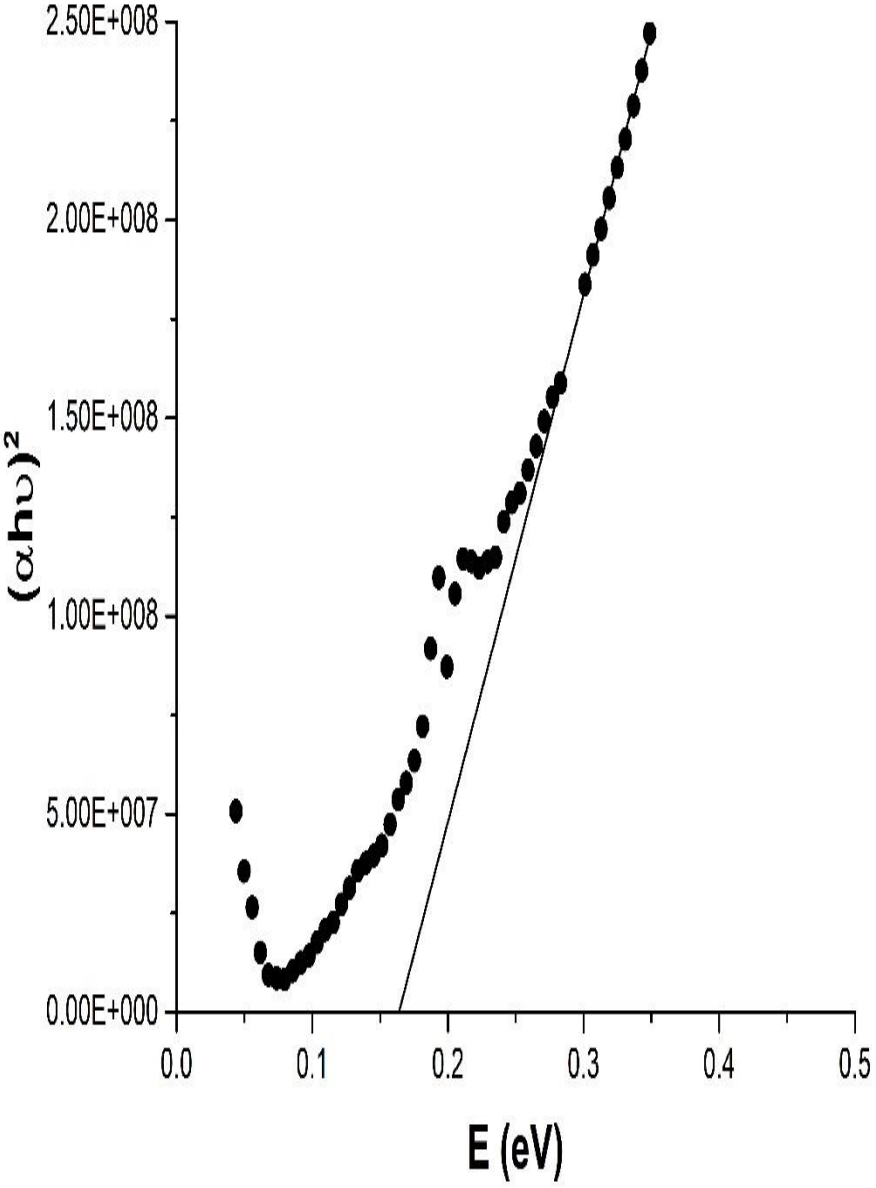

Figure-5 Plot of $(\alpha h\upsilon)^2$ versus $h\upsilon$ of $InSb_{0.97}Bi_{0.03}$ crystal

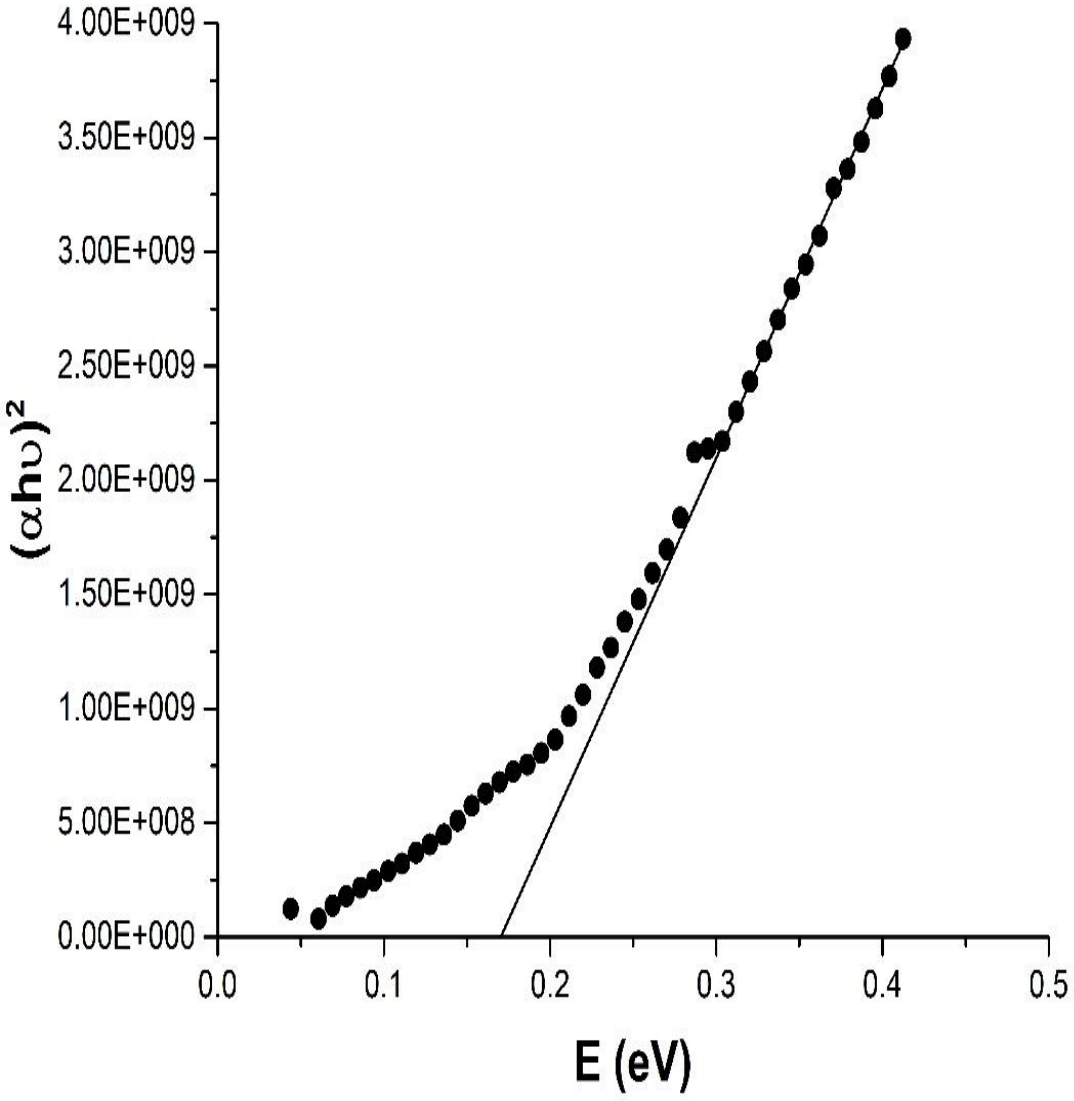

Figure-6 Plot of $(\alpha h\upsilon)^2$ versus $h\upsilon$ of $InSb_{0.96}Bi_{0.04}$ crystal

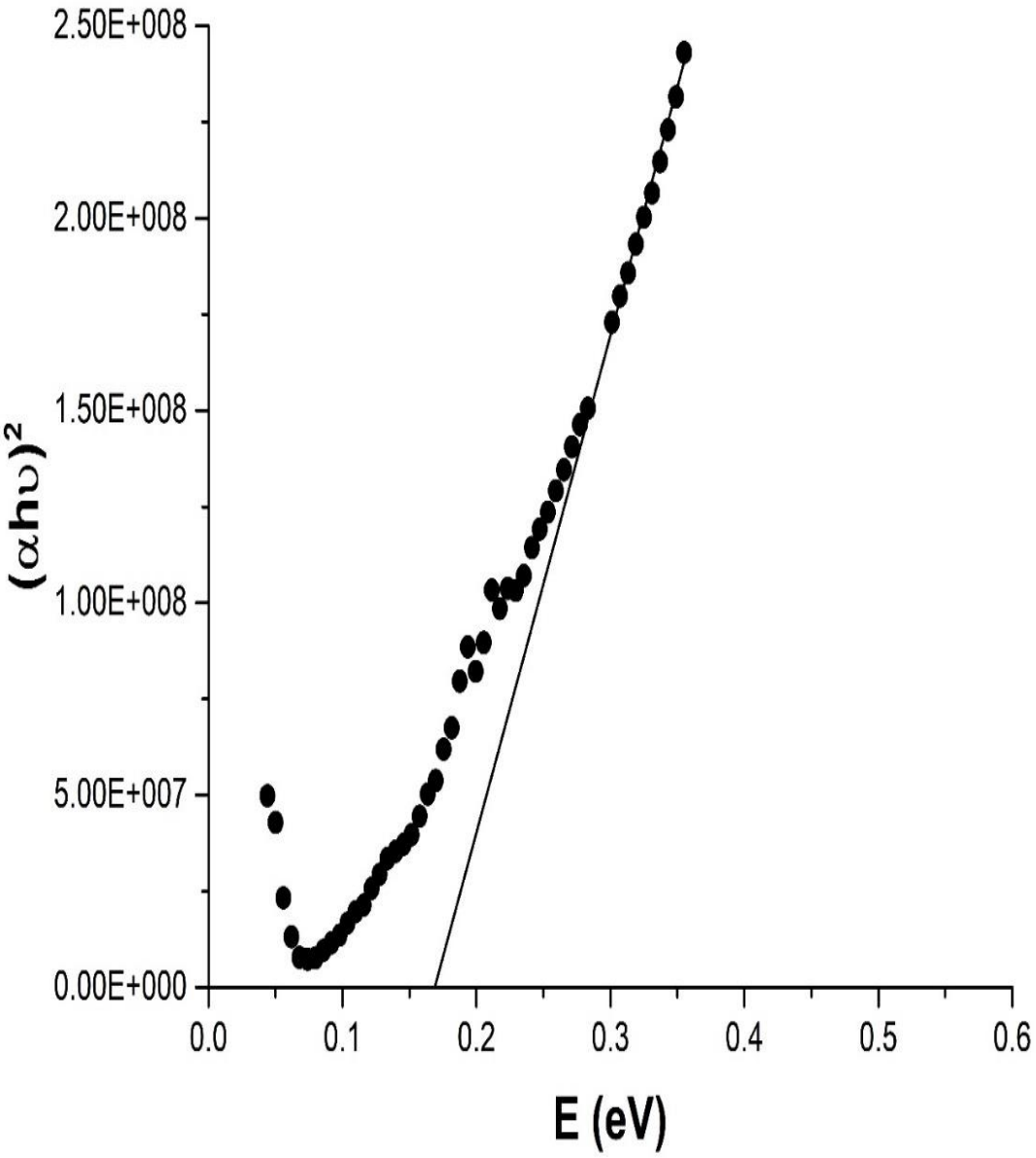

Figure-7 Plot of $(\alpha h\upsilon)^2$ versus $h\upsilon$ of $InSb_{0.95}Bi_{0.05}$ crystal

Table 2: Bandgap of InSb thin films

Sample	Thickness (Å)	Bandgap (eV)
InSb	525	0.243
	812	0.183
	1000	0.177
	1328	0.165
	1509	0.159

Table 3: Bandgap of $InSb_{0.97}Bi_{0.03}$ thin films

Sample	Thickness (Å)	Bandgap (eV)
$InSb_{0.97}Bi_{0.03}$	510	0.214
	819	0.167
	999	0.152
	1381	0.149
	1503	0.143

Table 4: Band gap of $InSb_{0.96}Bi_{0.04}$ thin films

Sample	Thickness (Å)	Bandgap (eV)
$InSb_{0.96}Bi_{0.04}$	505	0.208
	821	0.180
	1008	0.168
	1304	0.157
	1503	0.144

Table 5: Bandgap of $InSb_{0.95}Bi_{0.05}$ thin films

Sample	Thickness (Å)	Bandgap (eV)
$InSb_{0.95}Bi_{0.05}$	512	0.183
	801	0.176
	1003	0.153
	1320	0.149
	1512	0.144

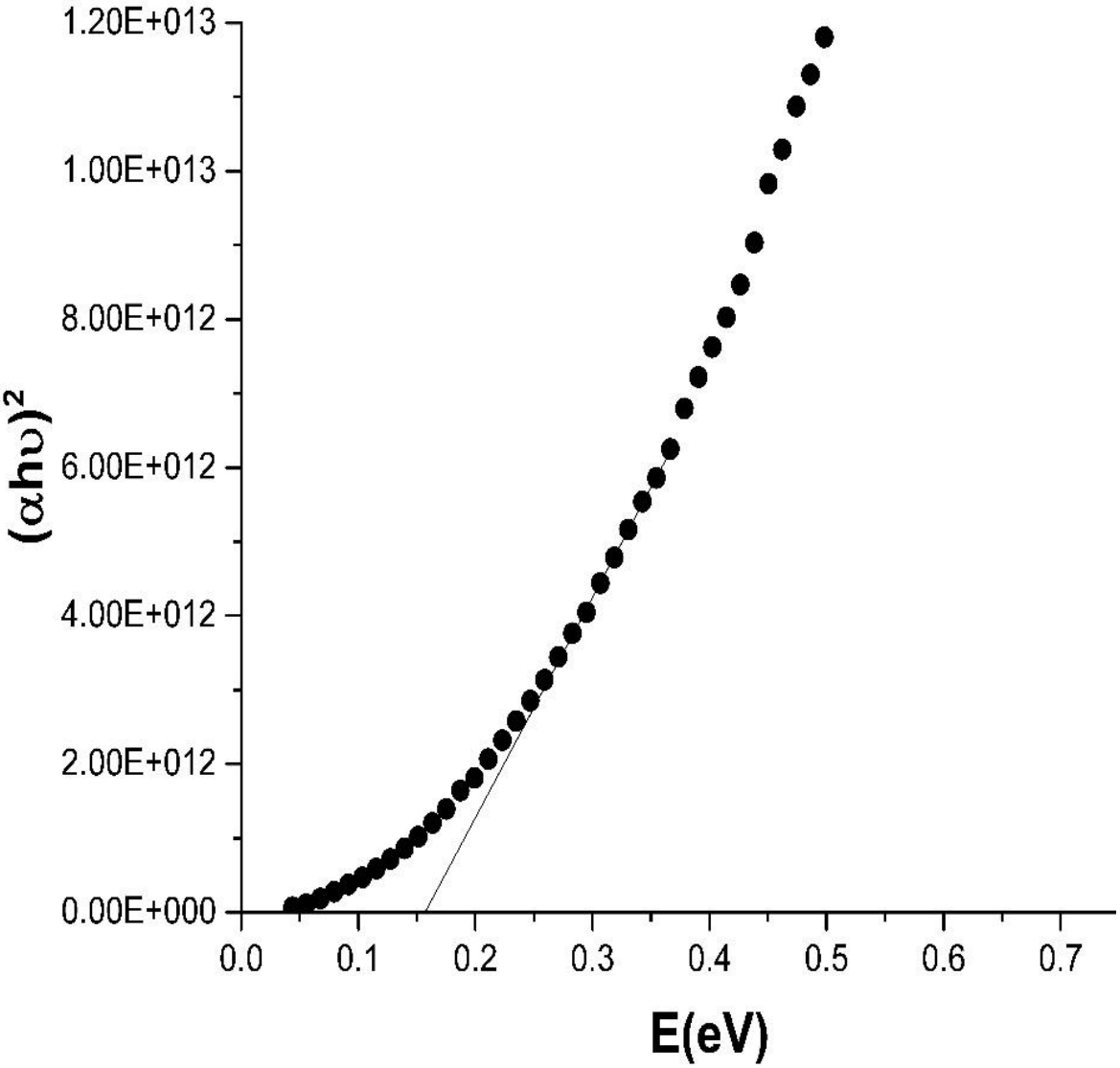

Figure-8 Plot of $(\alpha h\upsilon)^2$ versus $h\upsilon$ of InSb thin film

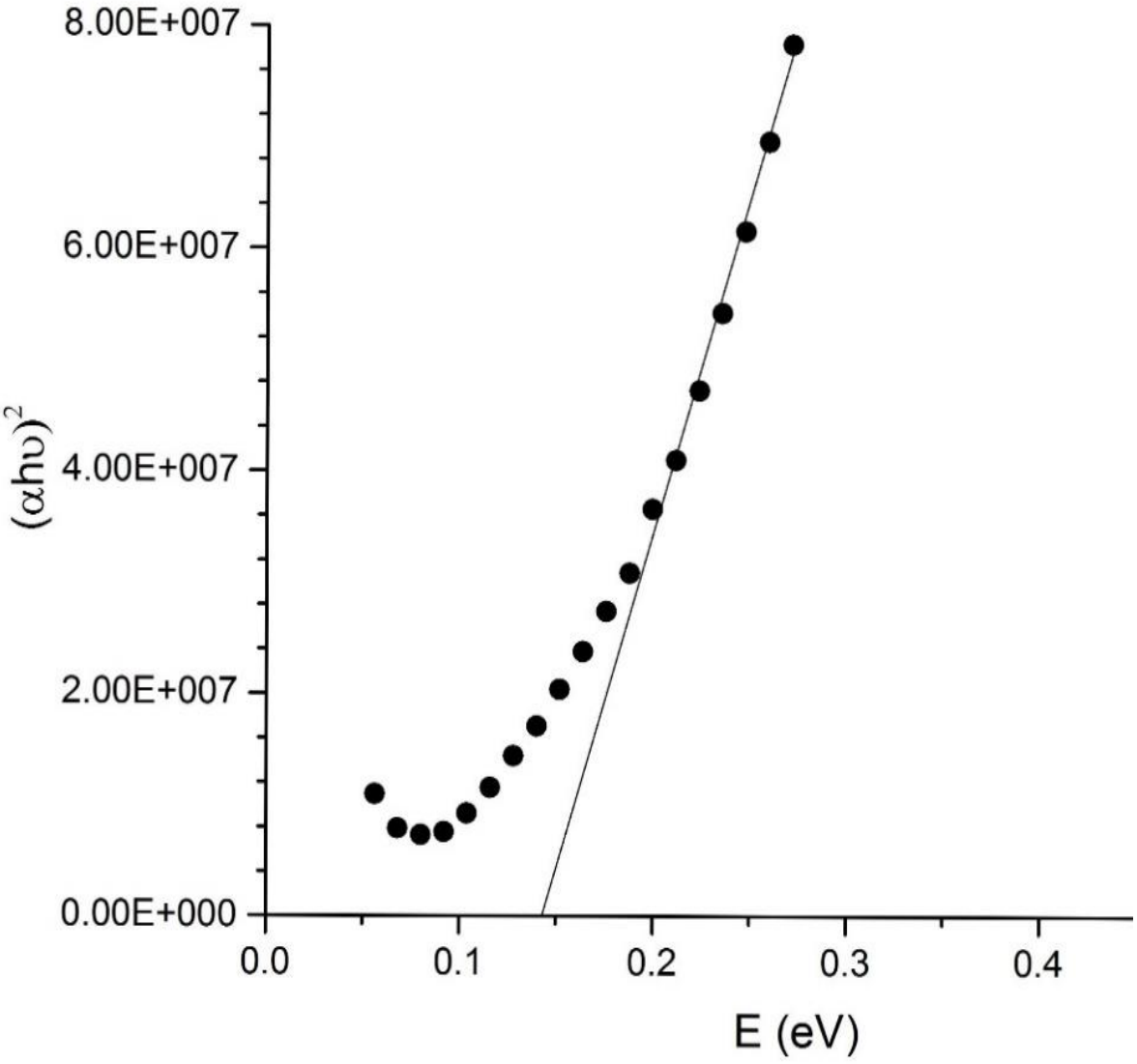

Figure-9 Plot of $(\alpha h\upsilon)^2$ versus $h\upsilon$ of $InSb_{0.97}Bi_{0.03}$ thin film

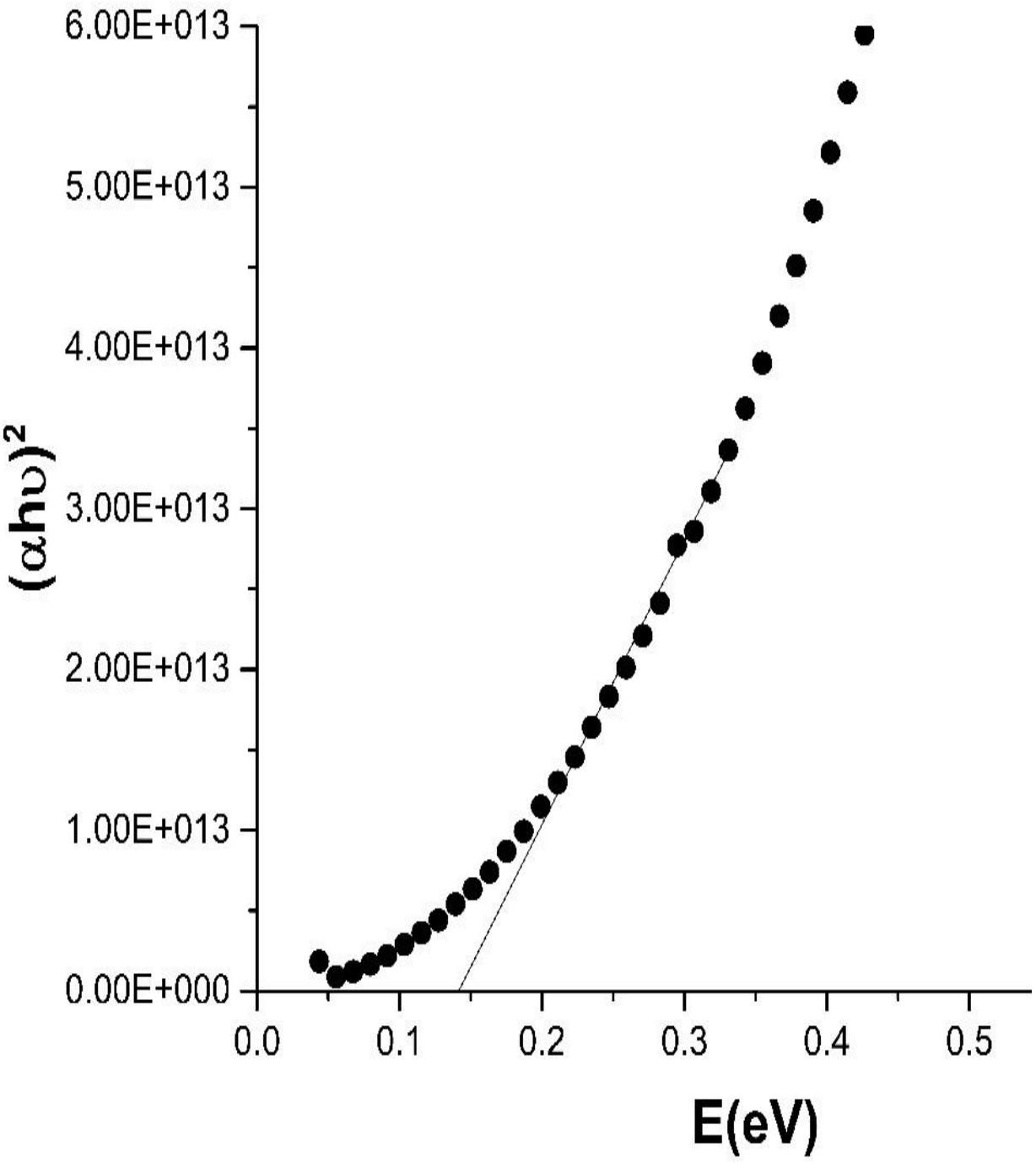

Figure-10 Plot of $(\alpha h\upsilon)^2$ versus $h\upsilon$ of $InSb_{0.96}Bi_{0.04}$ thin film

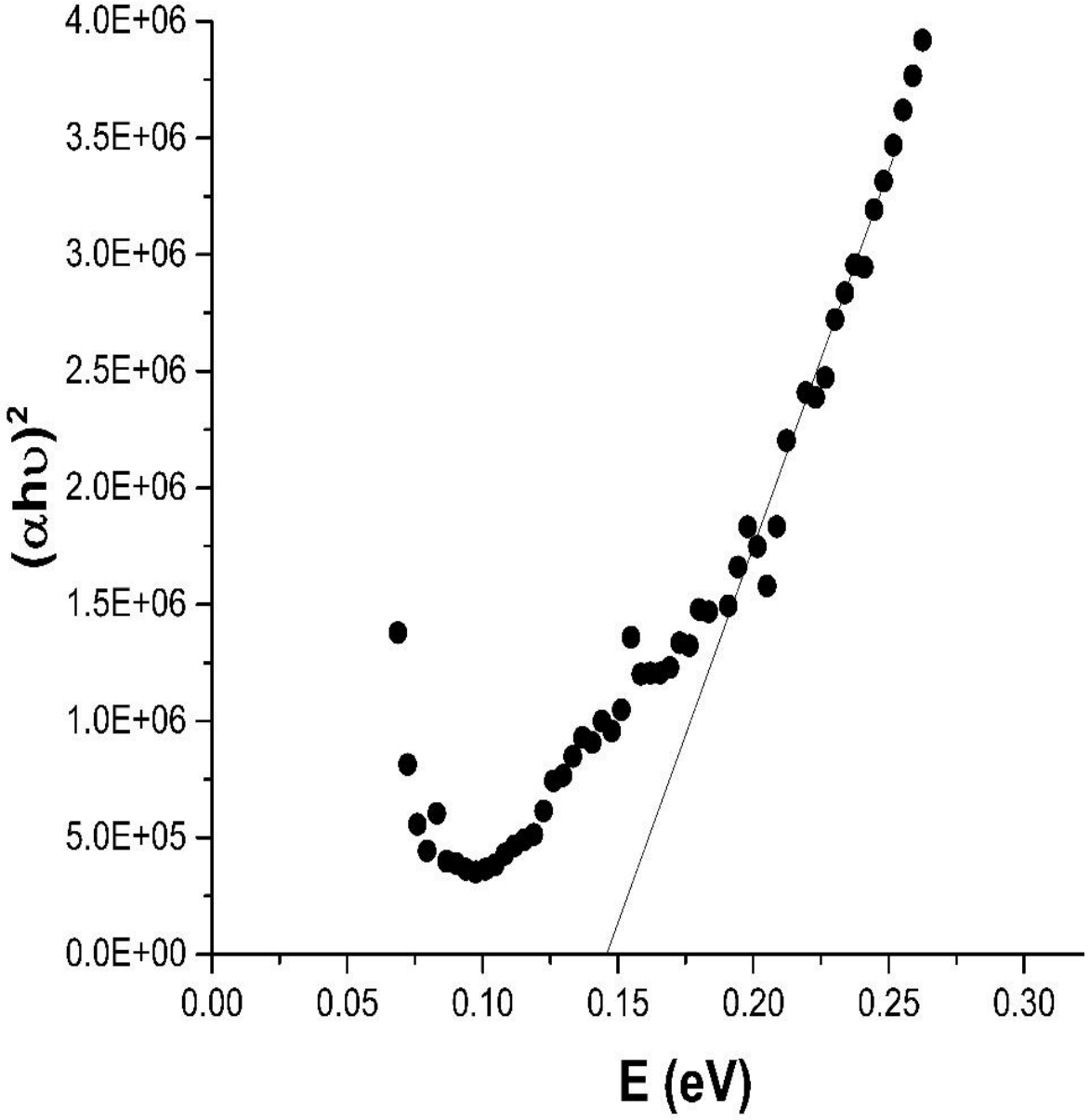

Figure-11 Plot of $(\alpha h\upsilon)^2$ versus $h\upsilon$ of $InSb_{0.95}Bi_{0.05}$ thin film

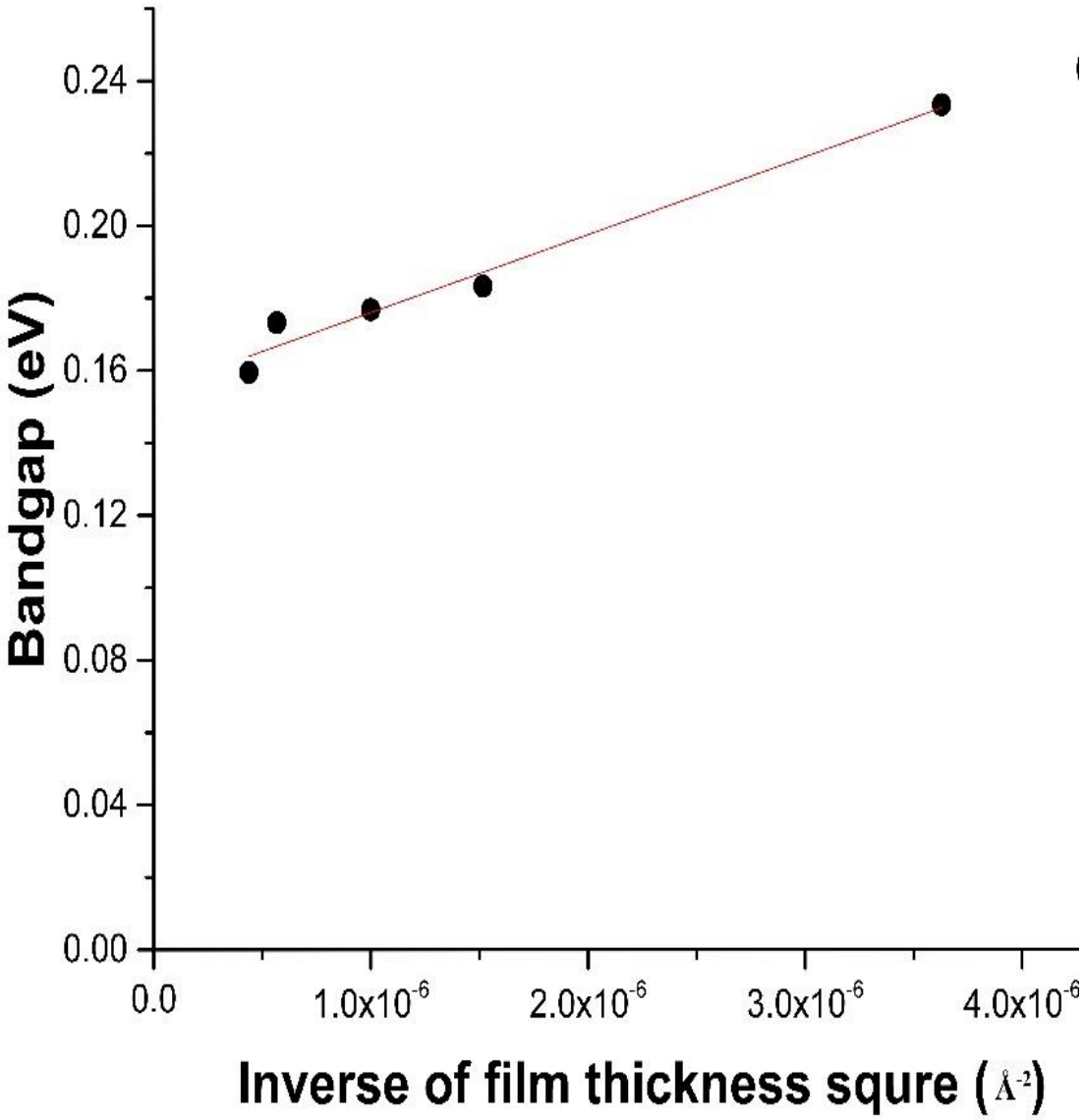

Figure-12 Plot of E_g versus$\frac{1}{t^2}$ of InSb thin film

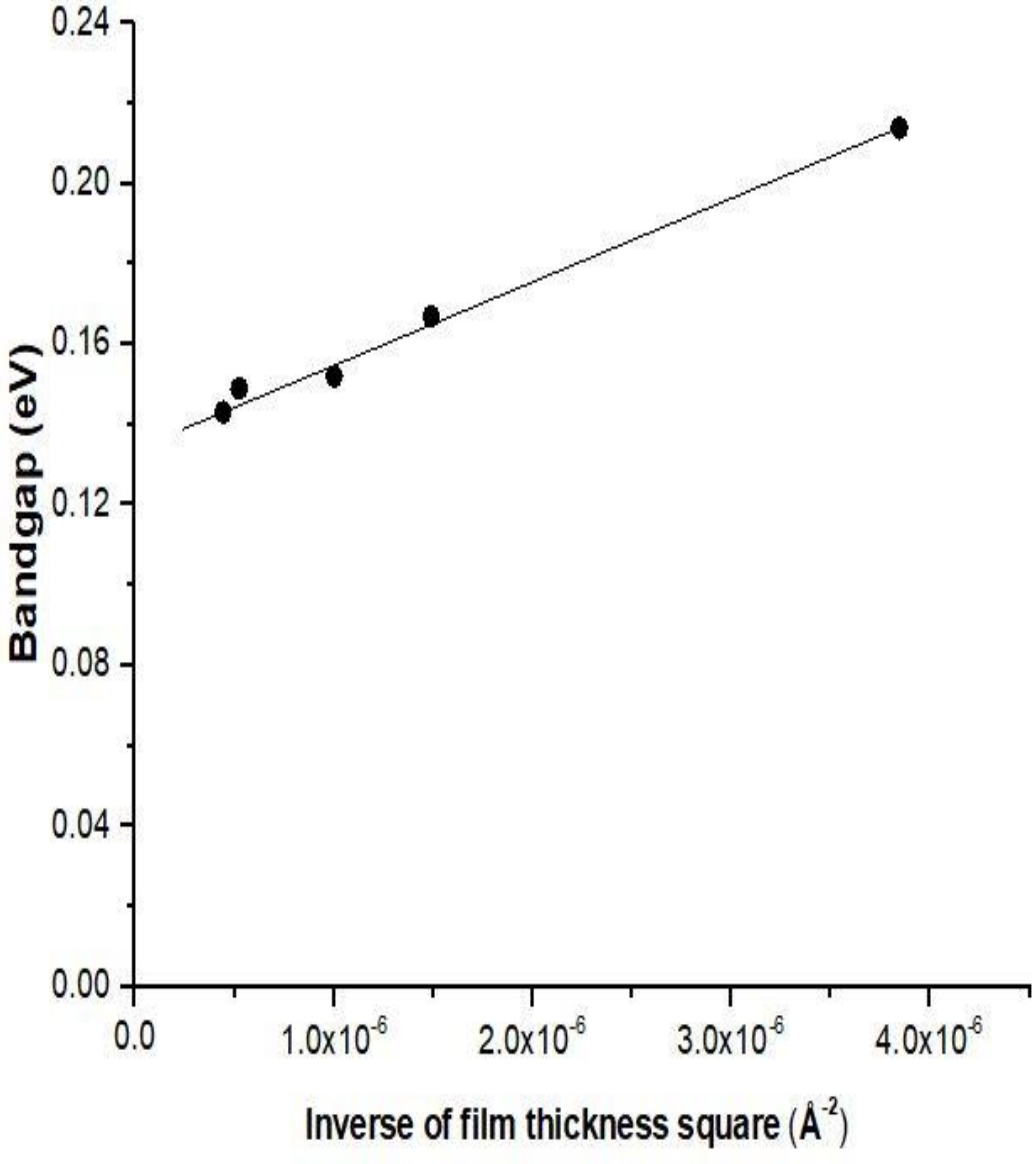

Figure-13 Plot of E_g versus$\frac{1}{t^2}$ of $InSb_{0.97}Bi_{0.03}$ thin film

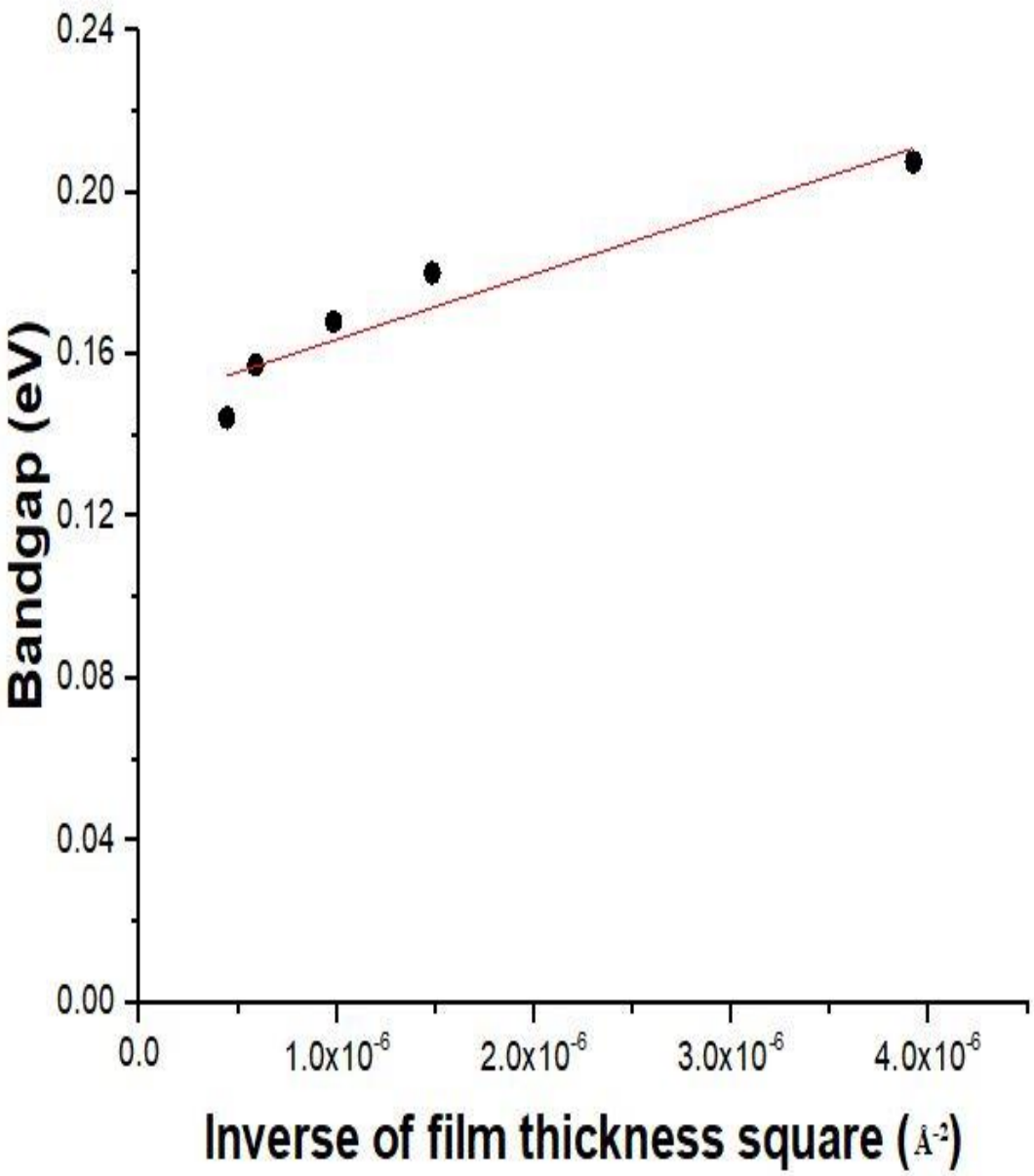

Figure-14 Plot of E_g versus$\frac{1}{t^2}$ of $InSb_{0.96}Bi_{0.04}$ thin film

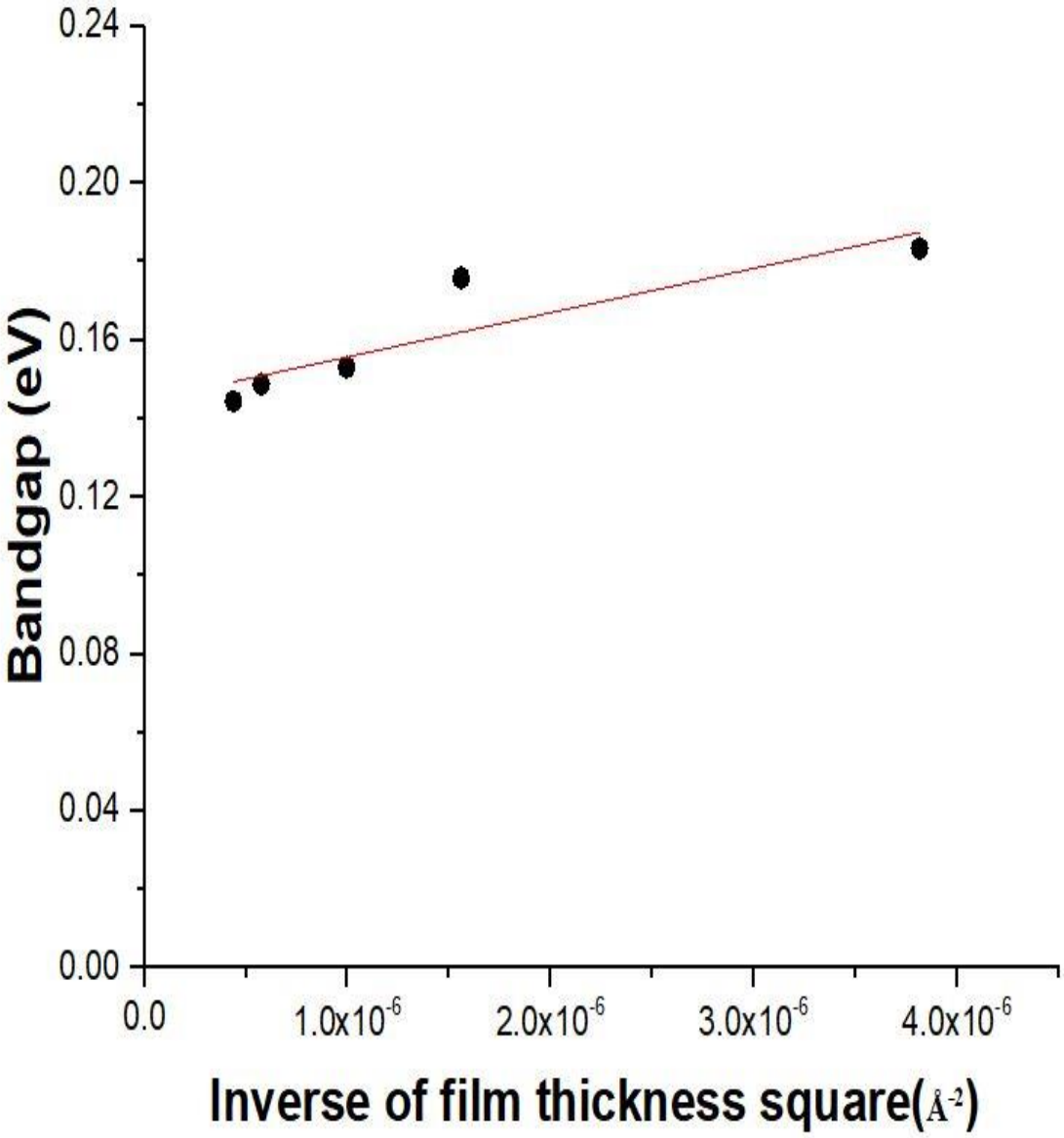

Figure-15 Plot of E_g versus$\frac{1}{t^2}$ of $InSb_{0.95}Bi_{0.05}$ thin film

It is well known that during the creation of thin films, a considerable number of dislocations are generated. The dislocation density also increases with increasing film thickness till the thickness tends to bulk form, in which case the density saturates assuming a bulk constant value. Dependence of dislocation density on film thickness has been so far not quantified but apparently the dependence would be complex. The dislocations being a major type of structural imperfection, the crystal lattice is under considerable disturbance. The disrupted or dangling bonds caused by dislocations bear their specific charge and space charge domains adversely affecting the band gap of the crystal.

The effect of the first granular structure that arises at the initial stage of film formation on the film properties, notably optical properties, reduces as the film thickness increases, but it does not disappear. Hence, thickness dependence sustains, though qualitatively. The optical properties, on the other hand, reflect the bulk structure's general trend. In principle, the electron energy in an infinitely thick crystal is a multivalue continuous function of its quasi-momentum, which is commonly described in terms of band structure. Whereas, in case of thin films, the quasi-momentum takes on discrete values in the direction of the thickness dimension. The uncertainty principle makes the energy spectrum of these carriers also a system of discrete energy levels. The effect of such levels on the forbidden energy band of a semiconductor is treated by Sandomiskii [23]. Accordingly, all the level of in the energy spectrum of a semiconductor get displaced by an amount ΔE, however small. If thermal energy smearing and diffuse scattering of carriers at the film surfaces are negligible, the energy shift would result in an increase in the band gap, altering the optical behaviour of the films. Obviously optical absorption in thinner films would be less than in the bulk form of the material. The band gap varies also with the crystallite size in thin films and the variation follows in accordance with a modified form of Stellar's formula [24]:

$$E = E_0 + C\,(X - f\,D)^2$$

Further, the grain size is approximately proportional to the film thickness [21]. So the quantity D in the above equation can be replaced with the the film thickness t and then E in the above expression can be said to be proportional to $(X - ft)^2$

The band gap is found to change in inverse proportion to the square of film thickness in the current study. As a result, it is safe to conclude that the observed band gap variation with thickness is not due to the above-mentioned phenomenon.

3.3 Photoresponse: $InSb_{1-x}Bi_x$ (x = 0.00, 0.03, 0.04, 0.05) films.

The grown thin films, $InSb_{1-x}Bi_x$ (x= 0.00, 0.03, 0.04, 0.05) showed photo conducting nature at zero biasing voltage and under illuminating condition. The photo response study of grown thin films were carried out under illumination of monochromatic LED having wavelength 670 nm of incident intensity of 100 mW.

Photo response of $InSb_{1-x}Bi_x$ (x=0.00, 0.03, 0.04, 0.05) thin films were carried out under the illumination of red monochromatic source and using Keithley-2400 SCS. For the measurement of I-V data, contacts were taken on the films using the conductive adhesive silver paste. The I-V characteristics of the grown films under dark condition are shown in figures 16, 17, 18 and 19 for $InSb_{1-x}Bi_x$ (x = 0.00, 0.03, 0.04, 0.05) respectively. From the graphs it can be concluded that devices show good ohmic nature. InSbBi was reported as very good material for IR detectors [25-26]. To check the applicability of the grown $InSb_{1-x}Bi_x$ (x = 0.00, 0.03, 0.04, 0.05) films in the same domain, I-V characteristics was carried out in illuminating condition. The I-V characteristics of the grown films under illuminating condition using LED having wavelength 670 nm are shown in figures20, 21, 22 and 23 for $InSb_{1-x}Bi_x$ (x = 0.00, 0.03, 0.04, 0.05) respectively. In the plots, (A) represents the dark current and (B) photocurrent. From the graphs it is clear that the grown Bi doped InSb thin films shows good photo response and hence proves its applicability as one of the preferred material for IR detector.

Main aim of photo response study is to validate the IR response of $InSb_{1-x}Bi_x$ (x = 0.00, 0.03, 0.04, 0.05) thin films. The obtained data shows the variation in resistance with the Bi doping amount. This variation is not homogenous because factors like sheet resistance, contact potential between silver pest and thin films, distance between two contacts etc. Further studies can be conducted to understand the resistivity variation.

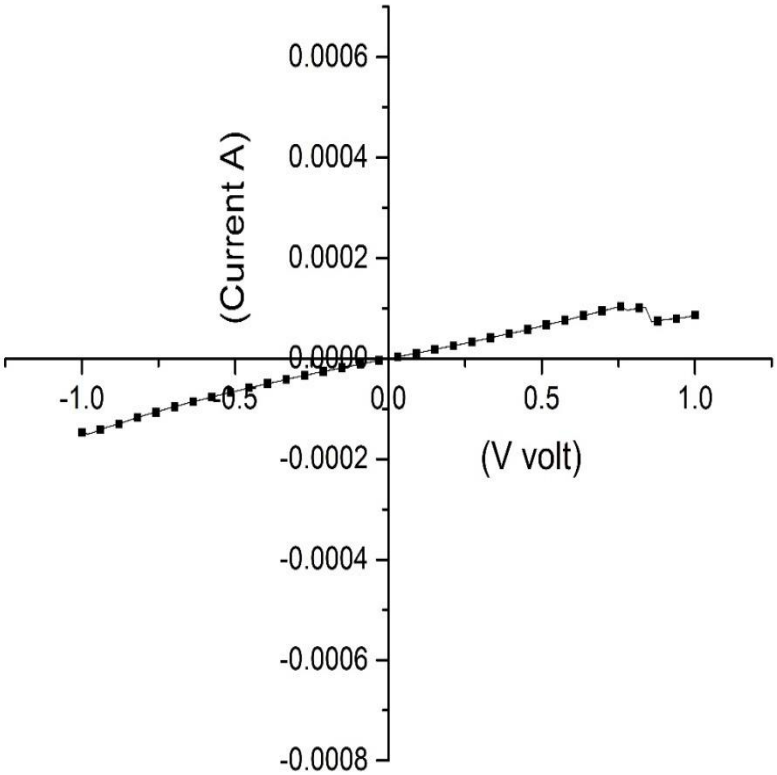

Figure -16 Plot of I-V characteristic of InSb thin film under dark condition

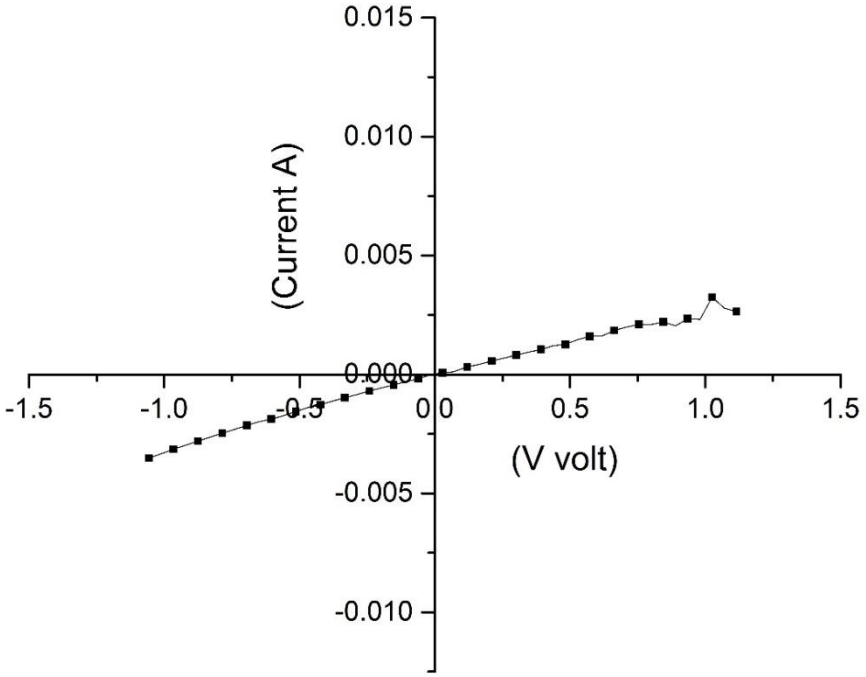

Figure-17 Plot of I-V characteristic of $InSb_{0.97}Bi_{0.03}$ thin film under dark condition

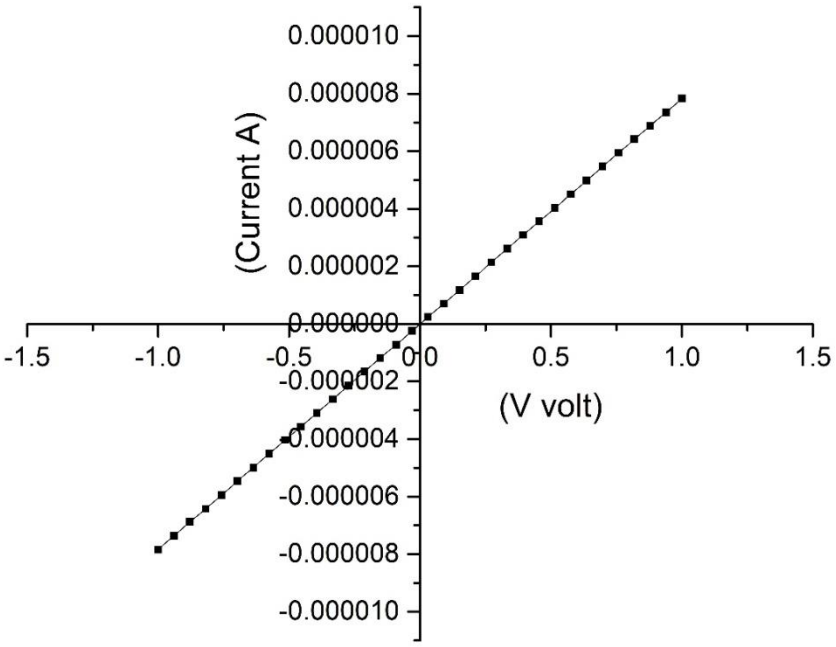

Figure-18 Plot of I-V characteristic of $InSb_{0.96}Bi_{0.04}$ thin film under dark condition

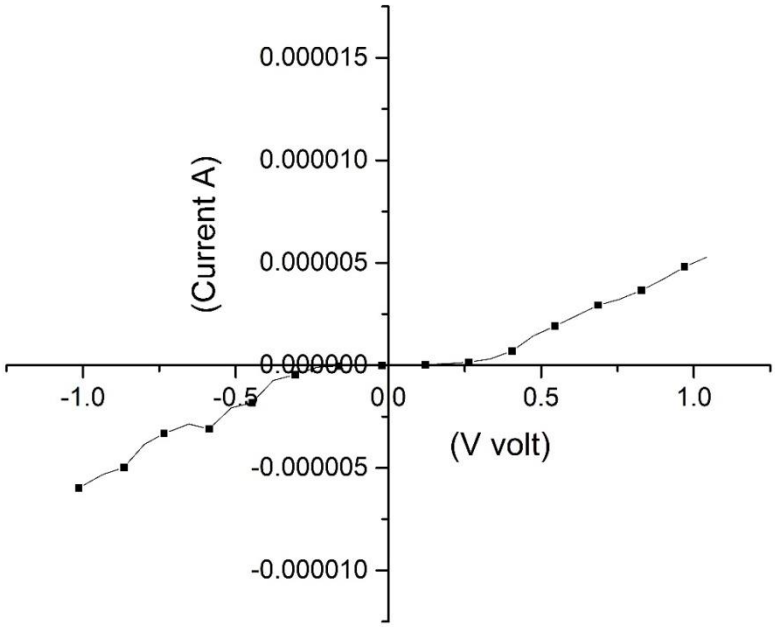

Figure-19 Plot of I-V characteristic of $InSb_{0.95}Bi_{0.05}$ thin film under dark condition

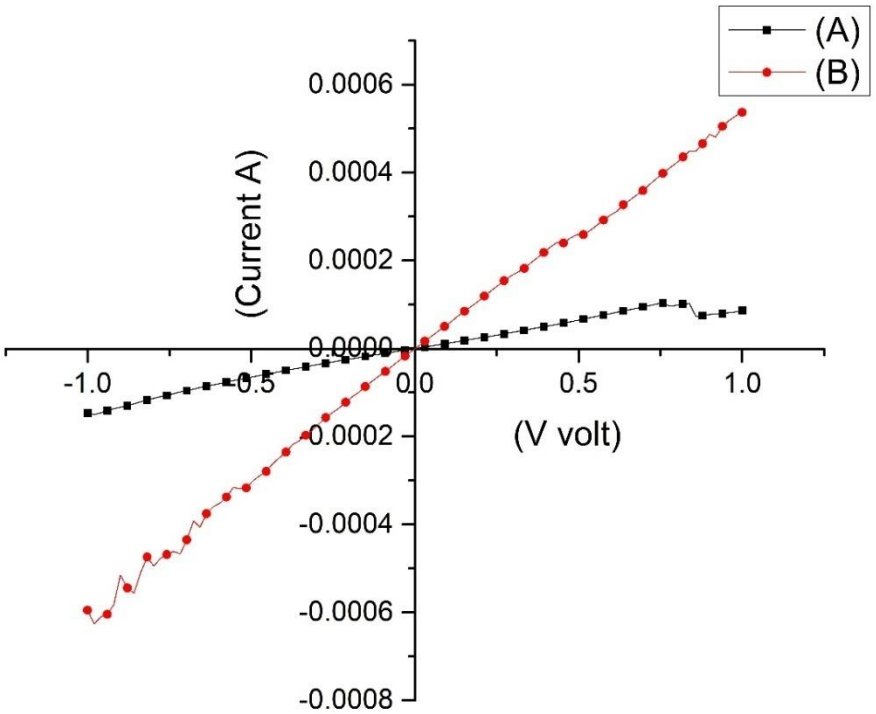

Figure-20 Plot of comparative I-V characteristic of InSb thin film under dark condition (A) and illuminating condition (B) (red light 670 nm)

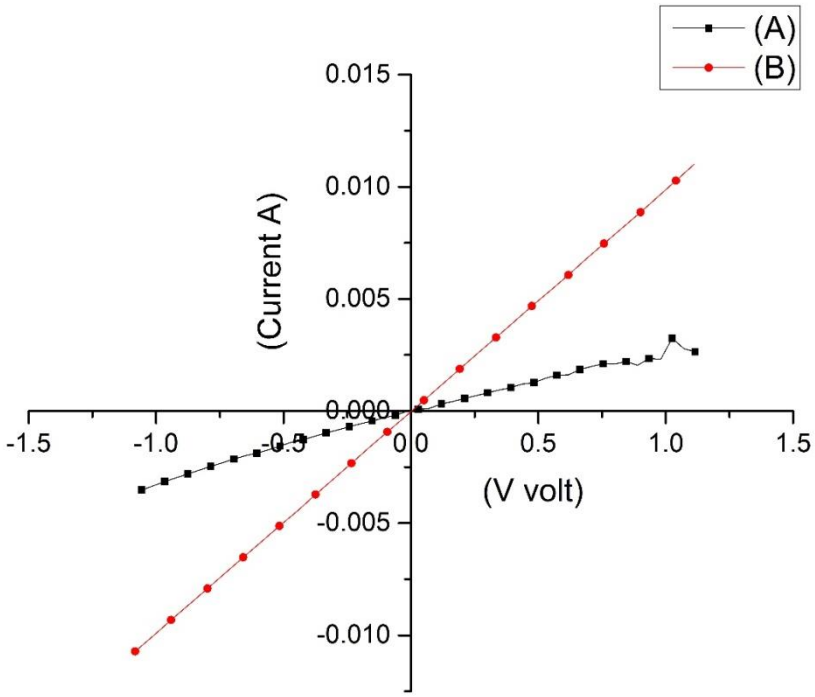

Figure-21 Plot of comparative I-V characteristic of $InSb_{0.97}Bi_{0.03}$ thin film under dark condition (A) and illuminating condition (B) (red light 670 nm)

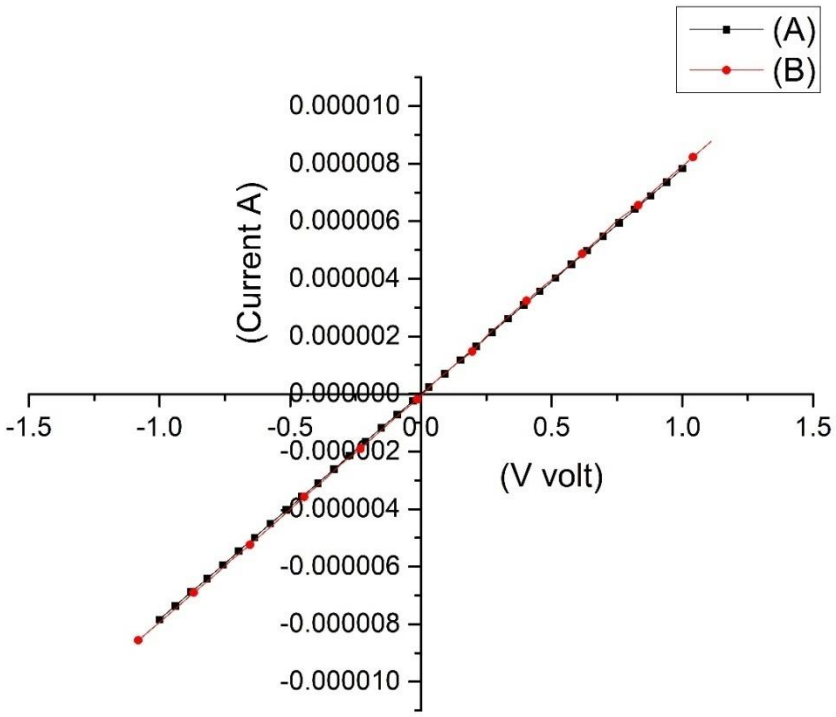

Figure-22 Plot of comparative I-V characteristic of $InSb_{0.96}Bi_{0.04}$ thin film under dark condition (A) and illuminating condition (B) (red light 670 nm)

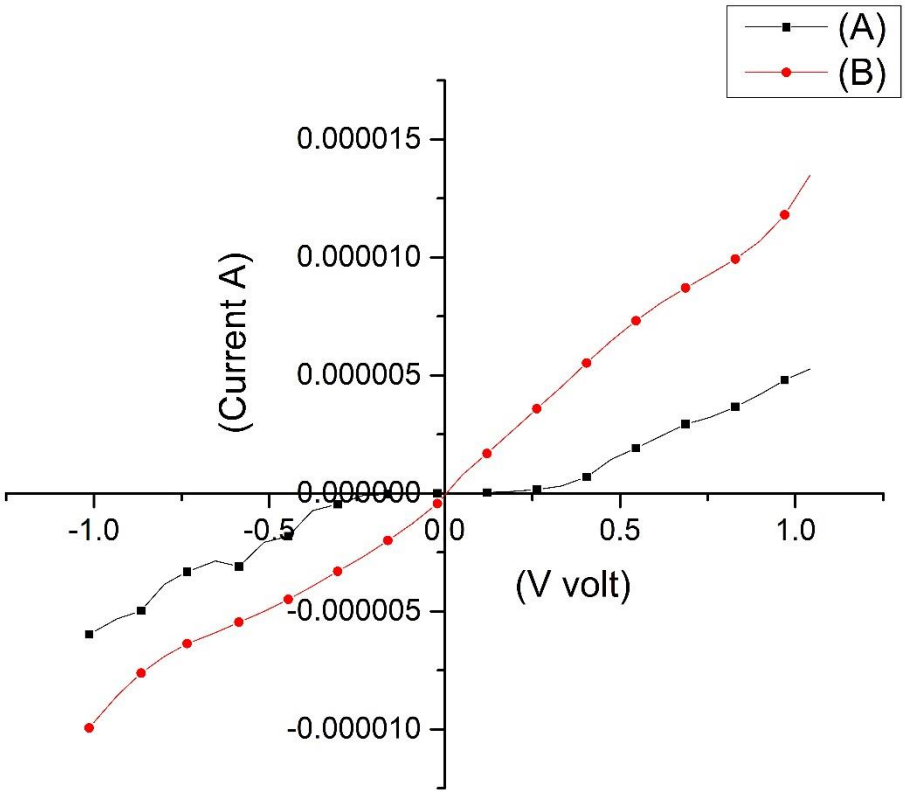

Figure-23 Plot of comparative I-V characteristic of $InSb_{0.95}Bi_{0.05}$ thin film under dark condition (A) and illuminating condition (B) (red light 670 nm)

IV. Conclusions:

1. The band gap of $InSb_{1-x}Bi_x$ (x= 0.03, 0.04, 0.05) crystals sizeably decreases compared to the band gap of pure InSb crystal.
2. The band gap of $InSb_{1-x}Bi_x$ (x= 0.00, 0.03, 0.04, 0.05) thin films is on an average 0.159 eV, 0.143 eV, 0.144 and 0.144eV, respectively (Direct type).
3. The band gap of $InSb_{1-x}Bi_x$ (x= 0.00, 0.03, 0.04, 0.05) thin films depends on film thickness.
4. The band gaps of smaller thickness thin films are larger than those of bulk ones.
5. The observed band gap dependency on thin film thickness implies that the optical transition is dominated by the quantum size effect within the thickness range examined.
6. Bi doped InSb thin films show good photoresponse.
7. $InSb_{1-x}Bi_x$ (x= 0.00, 0.03, 0.04, 0.05) thin films can be used as one of the preferred materials for IR detector.

References:

[1] O. S. Heavens: Optical properties of thin solid films, Butter Worths, London, (1955).

[2] O. S. Heavens: Rept. Progr. Physics 23 (1960) 1.

[3] P. H. Bering: Physics of thin films, Academic press, New York (1964) 69.

[4] H. E. Bennett and J. M. Bennettin: Physics of thin films, Academic press, New York 4 (1967) 1.

[5] D. S. Maske, M. Joshi, D. B. Gadkari, Int. J. Sci. and Res. Publ. 3(2), (2013).

[6] P. Mohan, S. M. Babu, P. Santhanaraghavan, P. Ramasamy, J. Mater. Sci. latters 20 (241-244) (2001).

[7] M. Oszwaldowski, T. Berus, J. Szade, K. Jozwiak, I. Olejniczak, P. Konarski, Cryst. Res. Technol. 36,8-10 (1155–1171) (2001).

[8] R. Bowers, R. W. Ure, Jr., J. E. Bauerle, A. J. Cornish, J. app. Physics, 30 (1959).

[9] S. Yamaguchi, T. Matsumoto, J. Yamazaki, N. Kaiwa, A. Yamamoto, App. Phy. Latters 87, 201902 (2005).

[10] S. M. Sze: Physics of Semiconductor devices: Wiley eastern limited New Delhi. (1979).

[11] Ben G. Streetman: Solid State electronic devices, Prentic – Hall of Indian Pvt. New Delhi. (1982).

[12] J. Barden, H. Hall and F. J. Balatt: Proceeding of the Conference on Photoconductivity, New York. 146 (1965).

[13] R. Tovar Barradas, C. Rincon, J. Genzalez and G. Sancher pertez: J. Phys. Chem. Solids 45 1185 (1984).

[14] Eva C. Freeman and Willam Paul: Physical Review B 20 716 (1979).

[15] J. Mendolia and d. Lemon: Phys. State Sol. (a) 97 601 (1986).

[16] R. H. Bube, A. L. F. Bruch: Fundamental of solar cell, Academic press, New York (1983).

[17] R. H. Bude: photoconductivity of solids, John Wiley and Sons Inc. New York (1960).

[18] K. P. Scharnhorst and H. R. Riedl: J. of Apply Phys. 43 5142 (1972).

[19] A. Rose: Phys. Rev. 97 322 (1955).

[20] P. H. Soni, S. R. Bhavsar, C. F. Desai, J. Mater. Sci. 38 1931 (2003).

[21] K. L. Chopra: Thin film phenomena McGraw-Hill, New York (1969).

[22] D. S. Chuu and M. D. Chang, Phys. Rev. B, 45 11805 (1992).

[23] V. B. Sandomirskii: Sov. Phys. JEPT 10 1630 (1963).

[24] J. C. Stallar: Physics Rev. 103 1931 (1956).

[25] S. N. Dwara, Amin H. Al- Khursan, Appl. Opt. Vol. 54, 9722 (2015).

[26] M. K. Rajpalke, W. M. Linhart, K. M. Yu, M. Birkett, J. Alaria, J. J. Bomphrey, S. Sallis, L.F. J. Piper, T. S. Jones, M. J. Ashwin, T. D. Veal, Appl. Phys. Letters 105, 212101 (2014)